J Neurophysiol 98: 2983–2991, 2007.
First published August 29, 2007; doi:10.1152/jn.00407.2007.

A Central Pattern Generator Producing Alternative Outputs: Phase Relations of Leech Heart Motor Neurons With Respect to Premotor Synaptic Input

Brian J. Norris,[1,2,*] Adam L. Weaver,[1,*] Angela Wenning,[1] Paul S. García,[1] and Ronald L. Calabrese[1]
[1]*Department of Biology, Emory University, Atlanta, Georgia; and* [2]*Department of Biological Sciences, California State University, San Marcos, California*

Submitted 10 April 2007; accepted in final form 27 August 2007

Norris BJ, Weaver AL, Wenning A, García PS, Calabrese RL. A central pattern generator producing alternative outputs: phase relations of leech heart motor neurons with respect to premotor synaptic input. *J Neurophysiol* 98: 2983–2991, 2007. First published August 29, 2007; doi:10.1152/jn.00407.2007. The central pattern generator (CPG) for heartbeat in leeches consists of seven identified pairs of segmental heart interneurons and one unidentified pair. Four of the identified pairs and the unidentified pair of interneurons make inhibitory synaptic connections with segmental heart motor neurons. The CPG produces a side-to-side asymmetric pattern of intersegmental coordination among ipsilateral premotor interneurons corresponding to a similarly asymmetric fictive motor pattern in heart motor neurons, and asymmetric constriction pattern of the two tubular hearts: synchronous and peristaltic. Using extracellular techniques, we recorded, in 61 isolated nerve cords, the activity of motor neurons in conjunction with the phase reference premotor heart interneuron, HN(4), and another premotor interneuron that allowed us to assess the coordination mode. These data were then coupled with a previous description of the temporal pattern of premotor interneuron activity in the two coordination modes to synthesize a global phase diagram for the known elements of the CPG and the entire motor neuron ensemble. These average data reveal the stereotypical side-to-side asymmetric patterns of intersegmental coordination among the motor neurons and show how this pattern meshes with the activity pattern of premotor interneurons. Analysis of animal-to-animal variability in this coordination indicates that the intersegmental phase progression of motor neuron activity in the midbody in the peristaltic coordination mode is the most stereotypical feature of the fictive motor pattern. Bilateral recordings from motor neurons corroborate the main features of the asymmetric motor pattern.

INTRODUCTION

Central pattern generator (CPG) networks (De Schutter et al. 2005; Marder and Calabrese 1996; Marder et al. 2005), consisting mainly of interneurons, produce an often complex temporal pattern of activity. This pattern is transferred synaptically by premotor interneurons to motor neurons to control rhythmic behavior. Particularly in invertebrates the key neuronal elements in CPG networks, including premotor elements, have been identified and their activity pattern defined. Moreover, in many cases the fictive motor pattern (activity of motor neurons) has been precisely determined. What is often lacking, however, is a precise description of the relative timing (coordination) of the activity of premotor interneurons and the motor neurons.

In the stomatogastric nervous system of crustaceans, the coordination of the fictive motor program with CPG activity has been precisely defined, but this is somewhat a special case because the motor neuron themselves are CPG elements and there a very few interneurons (Bucher et al. 2005, 2006; Marder and Bucher 2007). The stomatogastric CPGs are also not well suited to illuminate distributed CPGs that control and coordinate intersegmental motor outflow because of their local output. In the swimmeret CPG of crayfish (Mulloney and Hall 2007; Mulloney et al. 2006), and especially in the leech swimming CPG (Cang and Friesen 2002; Kristan et al. 2005), such quantitative descriptions of interneuron and motor neuron coordination are gradually emerging. Much progress is now being made in identifying the key neuronal elements that make up vertebrate pattern generators, and the fictive motor programs are often well described (Grillner et al. 2005; Kiehn 2006), although relative coordination has not been well quantified. In most preparations, it is simply too difficult to simultaneously record multiple premotor interneurons and motor neurons for melding the interneuron activity pattern with the motor pattern.

Here we focus on a quantitative assessment of the relative coordination of premotor interneurons and motor neurons in the leech heartbeat CPG as a necessary step for our long-range aim of a complete model of how a CPG controls intersegmental motor outflow. Such a quantitative assessment also allows us to determine variability across preparations. The observation that neuronal networks, and CPGs in particular, display a two- to fivefold range of intrinsic membrane currents and synaptic strengths while still producing stereotypical output (Marder and Goaillard 2006), begs the question of how variable such "stereotypy" is.

The heartbeat control system of the medicinal leech has been studied intensively for over three decades (for a recent review see Kristan et al. 2005). The leech has two tubular hearts running the length of the body and moving blood through its closed circulatory system (Krahl and Zerbst-Boroffka 1983; Thompson and Stent 1976a; Wenning et al. 2004a). The beating pattern (beat period 4–10 s) is asymmetric, with one heart generating high systolic pressure through a front-directed peristaltic wave (peristaltic coordination mode) along its length, and the other generating low systolic pressure through near-synchronous constriction (synchronous coordination mode) along its length. The peristaltic heart moves blood forward, whereas the synchronous heart has been hypothesized mainly

* These authors contributed equally to this work.
Address for reprint requests and other correspondence: R. L. Calabrese, Dept. of Biology, Emory University, 1510 Clifton Road N.E., Atlanta, GA 30322 (E-mail: ronald.calabrese@emory.edu).

The costs of publication of this article were defrayed in part by the payment of page charges. The article must therefore be hereby marked "*advertisement*" in accordance with 18 U.S.C. Section 1734 solely to indicate this fact.

to push blood into the peripheral circulation (Hildebrandt 1988; Wenning et al. 2004a) and supports rearward blood flow (Wenning and Meyer 2007). After about 20–40 beats (switch period ~100–400 s) the hearts switch roles (Krahl and Zerbst-Boroffka 1983; Thompson and Stent 1976a; Wenning et al. 2004a). This constriction pattern including the regular switches in coordination mode have been quantitatively described in detail (Wenning et al. 2004a).

Heart (HE) motor neurons occur as bilateral pairs in the midbody segmental ganglia 3 through 18 [designated HE(3)–HE(18)]. Each motor neuron innervates the segmental section of its ipsilateral heart tube and drives and entrains the beating of the heart in its segment (Maranto and Calabrese 1984a,b). In the isolated nervous system, the bursting discharge pattern of this ensemble of segmental motor neurons reflects well the segmental constriction pattern of the hearts and the switches in coordination mode (Wenning et al. 2004b). This asymmetric pattern of motor outflow has been quantified with respect to intersegmental phase relations, duty cycle, and intraburst spike frequency (Wenning et al. 2004b).

The central pattern generator for heartbeat consists of seven identified pairs of segmental heart (HN) interneurons located in the first seven midbody segmental ganglia [designated HN(1)–HE(7)]; one as yet unidentified pair of heart interneurons [designated HN(X) because its ganglion of origin is unknown] is known to exist (Calabrese 1977; Thompson and Stent 1976b,c) (Fig. 1*A*). Of the identified interneurons the HN(3) and HN(4) interneurons and the HN(6) and HN(7) interneurons are premotor (front and rear premotor interneurons, respectively) and make inhibitory synapses with ipsilateral motor neurons by a posterior directed axon (Fig. 1*B*) (Thompson and Stent 1976b). The unidentified HN(X) heart interneuron makes inhibitory synapses with ipsilateral HE(3)–HE(6) motor neurons. The heart interneurons interact with one another by inhibitory synapses and by electrical junctions that appear to be rectifying (Fig. 1*A*) (Calabrese 1977, 1979; Thompson and Stent 1976c). The first four pairs of interneurons [HN(1)–HN(4)] form an oscillatory core that paces beat timing for the entire pattern generator network. This core timing network has been examined in detail (Masino and Calabrese 2002a,b,c) and modeled extensively (Hill et al. 2002; Jezzini et al. 2004). The timing network is linked to the rear premotor interneurons through direct ipsilateral electrical connections and indirectly through bilateral inhibitory connections from the HN(5) heart interneuron pair (Fig. 1*B*). The HN(5) interneurons are called switch interneurons because bilateral recordings (Calabrese and Peterson 1983; Lu et al. 1999) show one active in rhythmic bursts and one inactive with reciprocal switches in activity state every 20–40 heartbeat cycles. The inactive state is caused by a persistent leak-like conductance—reversal potential near −60 mV—that suppresses spike activity (Gramoll et al. 1994). The active state of the switch interneuron gives rise to the synchronous coordination mode and the inactive state to the peristaltic coordination mode (Calabrese 1977; Calabrese and Peterson 1983). The switch interneurons do not appear to be able to switch autonomously and it is hypothesized that they are under control of a switch oscillator extrinsic to the known heart interneurons (Lu et al. 1999).

Recently we have completed a quantitative description of the activity pattern (phase relations, duty cycle, and intraburst spike frequency) of all the premotor interneurons [including the HN(X) interneurons] and of the switch interneurons using extracellular recording techniques that minimally perturb network activity and permit relatively long-term recording (Norris et al. 2006). This analysis confirmed that switches in coordination are associated with reciprocal switches in the activity of the switch interneurons. The result of the change in switch interneuron activity is that the phase relations of the HN(6), HN(7), and HN(X) premotor interneurons shift with respect to the HN(3) and HN(4) premotor interneurons that are part of the phase-invariant timing network core (Fig. 1*A*). Thus we have a complete quantitative description of the temporal pattern of CPG fictive output onto motor neurons and a complete description of the fictive pattern of motor neuron firing.

Here we use extracellular recording techniques that minimally perturb network activity to assess quantitatively the phase relations of the fictive pattern of segmental motor neuron firing with the fictive pattern of CPG premotor interneuron firing, thus providing the temporal link between these two fictive patterns. Moreover, we also assess the variability in these two patterns across preparations and compare this variability to variability in the constriction patterns of the two hearts.

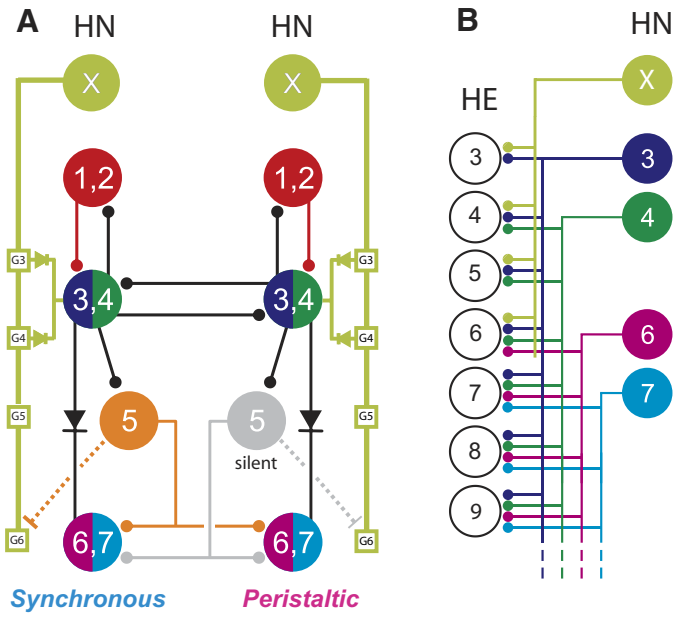

FIG. 1. Network diagrams for the leech heartbeat central pattern generator (CPG: heart interneuron circuit) and the CPG output to associated heart motor neurons. *A*: circuit diagram showing synaptic connections among interneurons of the heartbeat CPG. *B*: hemilateral circuit diagram showing all the premotor heart (HN) interneurons of the CPG [identified HN(3), HN(4), HN(6), HN(7), and unidentified HN(X)] and their pattern of synaptic connections to ipsilateral motor neurons (HE) in HE(3)–HE(9). In both panels, large colored circles are cell bodies and associated input processes. Lines indicate cell processes, small colored/black circles indicate inhibitory chemical synapses, small boxes along the HN(X) interneurons' axons in G3–G6 are putative spike initiation sites, and diodes indicate rectifying electrical synapses. Dashed process extending from the G5 interneuron to the G6 initiation site of the HN(X) interneuron indicates an indirect excitatory pathway (Norris et al. 2006). For simplicity in the CPG diagram of *A*, cells with similar input and output connections and function are lumped. Standard colors for the identified interneurons are used (see METHODS for color code); e.g., lime green is used for the X interneuron. HN(X) interneuron is defined as one that gives rise to matched IPSPs in ipsilateral G3–G6 heart motor neurons and rectifying electrical coupling potentials in ipsilateral G3 and G4 interneurons (Calabrese 1977).

METHODS

Animals and solutions

Leeches (*Hirudo* sp) (Siddall et al. 2007) were obtained from commercial suppliers (Leeches USA, Westbury, NY and Biopharm, Charleston, NC) and maintained in artificial pond water at 15°C. After the animals were anesthetized in cold saline, chains of ganglia were dissected consisting of the head brain (HB) to at least midbody ganglion 15 (G15) for recording the heart interneuron and heart motor neuron activity rhythms. The preparations were pinned (ventral surface up) in 60-mm petri dishes lined with Sylgard (Dow Corning, Midland, MI). Ganglia in which heart interneurons or heart motor neurons were to be recorded were desheathed using fine scissors or microscalpels. The preparation was superfused continuously with normal leech saline containing (in mM): 115 NaCl, 4 KCl, 1.8 $CaCl_2$, 10 glucose, and 10 HEPES buffer, adjusted to pH 7.4 with NaOH, at 1–2 ml/min (bath volume 6–8 ml). Heart motor neurons and interneurons were identified based on soma size, soma location in the ganglion, and ultimately identified by their characteristic bursting activity (e.g., Fig. 2). Previous experience has indicated that the heart interneuron HN(X) activity pattern associated with synchronous coordination is sensitive to prolonged dissection and extensive desheathing of ganglia (Norris et al. 2006); thus when recording the coordination of front motor neurons with premotor interneurons all attempts were made to keep dissections <1 h and to minimize the number of ganglia desheathed. Moreover, those preparations where the phasing of front motor neurons never switched out of the peristaltic state during the course of an experiment (often despite documented switches in the identified rear premotor interneurons) were discarded.

Extracellular recording techniques

For extracellular recordings from heart interneurons and heart motor neurons, we used suction electrodes filled with normal saline. Electrodes were pulled on a Flaming/Brown micropipette puller (P-97, Sutter Instrument, Novato, CA) from borosilicate glass (1 mm OD, 0.75 mm ID; A-M Systems, Carlsborg, WA) and placed in a suction electrode holder (E series, Warner Instruments, Hamden, CT). To ensure a tight fit between the cell and electrode, the electrode tips had a final inner diameter of about 20 μM for interneurons and of about 30 μM for motor neurons, approximately the diameter of heart interneuron/motor neuron somata, respectively. The electrode tip was brought in contact with the cell body and light suction was applied using a syringe until the entire cell body was inside the electrode. Extracellular signals were monitored with a differential AC amplifier (model 1700, A-M Systems) at a gain of 1,000 with the low- and high-frequency cutoffs set at 100 and 1,000 Hz, respectively. Noise was reduced with a 60-Hz notch filter and a second amplifier (model 410, Brownlee Precision, Santa Clara, CA) amplified the signal appropriately for digitization.

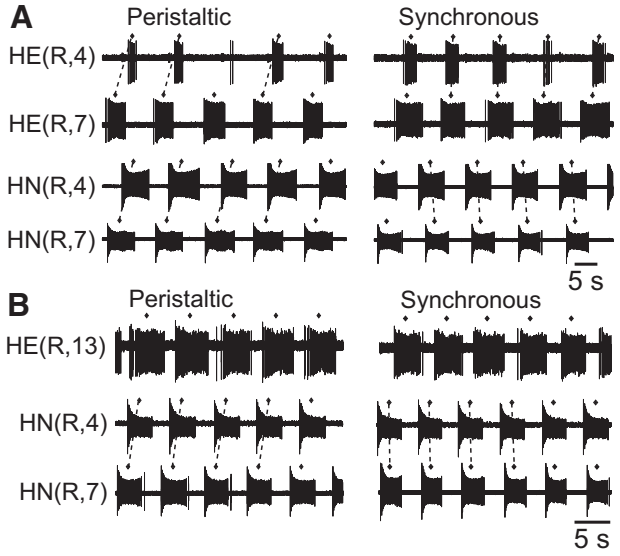

FIG. 2. Coordination of front and rear heart motor neurons with the heartbeat CPG. Shown are extracellular recordings from 2 front (*A*) and a rear heart motor neuron (*B*) with the ipsilateral phase reference HN(4) interneuron in both peristaltic and synchronous coordination mode. Black diamonds indicate the middle spike of each burst and dashed lines are provided to facilitate observation of relative phasing. Coordination mode is indicated by the relative phasing of the ipsilateral HN(4) and HN(7) interneurons. *A* and *B* from different preparations.

Data acquisition and analysis

Data were digitized (sampling rate 3.3 kHz) using a digitizing board (Digi-Data 1200 Series Interface, Axon Instruments, Foster City, CA) and acquired using pCLAMP software (Axon Instruments) on a personal computer (PC).

Determining the heart interneuron/motor neuron activity pattern and phase relations

For analysis of extracellularly recorded spike trains to determine the heart interneuron/motor neuron activity pattern and phase relations 61 total preparations were used, 29 in which HE(3)–HE(7) motor neurons were recorded and 32 in which HE(8)–HE(18) motor neurons were recorded. Spike detection was carried out in Spike2 (Cambridge Electronic Design, Cambridge, UK) using methods similar to those outlined previously (Norris et al. 2006). Briefly, spikes were detected with a discrimination window. When voltage crossed a lower threshold value, but did not exceed an upper threshold, a spike event was detected and was indicated by a raster point above the spike. The upper threshold eliminated transient artifacts in the recording. To prevent multiple detection of the same spike, a refractory period (20 ms), during which spikes could not be recognized, was applied after each detected event. To ensure that all spikes were detected, the refractory period was considerably shorter than the shortest interspike interval (~50 ms).

In most recordings, heart interneuron/motor neuron spikes were easily discernable by eye because they were the only units present in the recording and spike amplitude remained constant over periods of 20 min to ≥1 h. In a minority of the preparations, the extracellular recordings would lose suction and have a signal that progressively grew weaker before the suction was reestablished. In these cases, the signal was low-pass filtered and differentiated to reduce noise levels relative to the signal. Then, spike thresholds were varied according to the signal levels.

For analysis of burst characteristics, period, duty cycle, and intraburst spike frequency, spikes were grouped into bursts as follows. After an interburst interval (≥1 s) elapsed without any spikes detected, the next spike event was identified as the first spike of a burst. Subsequent spikes with interspike intervals less than the interburst interval were grouped into that burst. To eliminate the effects of occasional stray spikes in heart motor neurons and interneurons, groups of fewer than five spikes were not considered as bursts. The middle spike in each burst was indicated by a symbol above the burst. Herein, specific symbols and specific colors are used in traces, graphs, and diagrams to represent heart interneurons from specific midbody ganglia: *diamond/red*, HN(1)/HN(2) interneurons; *circle/dark blue*, HN(3) interneurons; *asterisk/dark green*, HN(4) interneurons; *open circle/orange*, HN(5) interneurons; *triangle/magenta*, HN(6) interneurons; *square/cyan*, HN(7) interneurons; and *cross/lime green*, HN(X) interneurons. Black diamonds are used for all phase markers when color was not used.

We then calculated burst period (T), phase (ϕ), duty cycle (D), and intraburst spike frequencies (see following text) for each recorded cell. Every effort was made to maximize the number of representative bursts analyzed within a coordination mode. Bursts were not included if the neuron showed signs of injury, had one to two cycles of disrupted patterning, or if one of the heart interneurons was no longer following 1:1 with the other heart interneurons. For this analysis, an average of 20.53 ± 1.10 (SD) cycles was used per preparation for each coordination mode with a minimum number of five cycles used (usually $n \geq 12$ consecutive bursts). In a few preparations, one or more heart interneurons/motor neurons were insufficiently inhibited (or slightly damaged in the dissection and/or the recording) such hat they continued to fire at very low rates (<5 Hz) during their inhibited phase. In this case, as few as possible detected spikes were removed around troughs in the instantaneous spike frequency to achieve a sufficient interburst interval (1 s) for burst detection. To represent the burst period of the entire central pattern generator, the burst period of an HN(4) interneuron [or an HN(3) interneuron in the small number of cases where no HN(4) interneuron was recorded] was determined.

Burst period was defined as the interval in seconds from middle spike to middle spike of consecutive bursts and the mean burst period (T_i) was determined for each cell (i) (ganglion index for an interneuron or motor neuron). The unilateral (or relative) phase of a given heart motor neuron (or interneuron) was defined on a cycle-by-cycle basis as the time (t) difference between the middle spike of its burst (t_i) and the middle spike of the preceding ipsilateral HN(4) heart interneuron's burst (t_4; ipsilateral phase reference cell). The time difference was then normalized to the burst period of the ipsilateral phase reference cell and expressed as a decimal number (between 0 and 1): $\phi_i = \Delta t_{i-4}/T4$. A phase of 1.0/0.0 indicated a cell with no phase difference relative to the phase reference, the ipsilateral HN(4) heart interneuron, whereas a 0.50 phase difference indicated an antiphasic relationship. To unify phase calculations in the two different modes or in bilateral recordings, the unilateral (relative) phase calculated in the synchronous coordination mode was offset by 0.511, corresponding to the empirically measured phase difference (0.5106 ± 0.0216; $n = 10$) in bilateral recording between the peristaltic HN(4) interneuron (defined as 0.0 phase) and the synchronous HN(4) interneuron [i.e., the peristaltic HN(4) interneuron became the absolute phase reference] (Norris et al. 2006). All phases were expressed modulo 1. This adjustment allowed a complete bilateral assessment of motor neuron phase with respect to the HN(4) interneurons (absolute phase). Phases calculated for individual experiments were then averaged across preparations to obtain a mean phase. To calculate the duty cycle and for the purpose of phase box plots we also calculated the mean absolute phase of the first and the last spikes of the bursts, as earlier for the middle spike. Mean duty cycle (D) was then determined by subtracting the mean first spike phase from the mean last spike phase, adding 1, and taking the value modulo 1. If this number was negative, 1 was added. Duty cycle was thus calculated without SD and represents the fraction of the burst period occupied by the burst. The mean duty cycle for each interneuron/motor neuron was then displayed as a box plot (normalized burst duration) in the bilateral phase diagrams subsequently described. These phase diagrams were then integrated with similarly constructed bilateral phase diagrams for the identified premotor interneurons and the switch interneurons (Fig. 4 in Norris et al. 2006) and for the HN(X) interneurons (Fig. 10 in Norris et al. 2006).

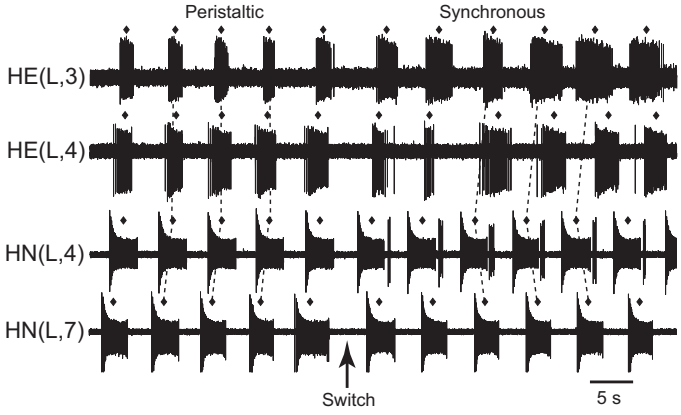

FIG. 3. Coordination of HE(3) and HE(4) heart motor neurons with the heartbeat CPG. Shown are extracellular recordings from HE(3) and HE(4) heart motor neurons with the ipsilateral phase reference HN(4) interneuron across a switch (arrow) from peristaltic to synchronous coordination mode. Black diamonds indicate the middle spike of each burst and dashed lines are provided to facilitate observation of relative phasing. Coordination mode is indicated by the relative phasing of the ipsilateral HN(4) and HN(7) interneurons. Across the switch the motor neurons shift phase both with respect to each other and to the ipsilateral HN(4) phase reference.

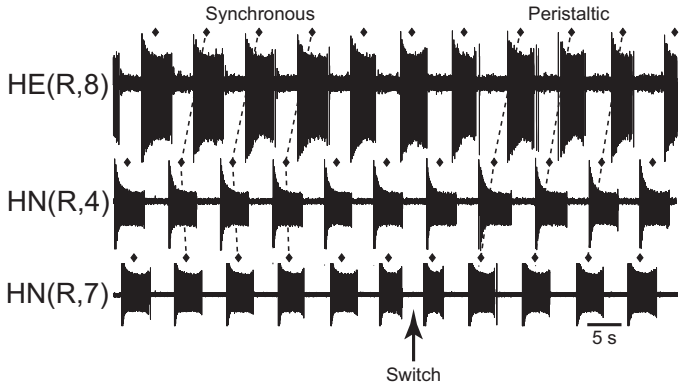

FIG. 4. Coordination of an HE(8) heart motor neuron with the heartbeat CPG. Shown are extracellular recordings from an HE(8) heart motor neuron with the ipsilateral phase reference HN(4) premotor interneuron and the HN(7) premotor interneuron across a switch (arrow) from synchronous to peristaltic coordination mode. Black diamonds indicate the middle spike of each burst and dashed lines are provided to facilitate observation of relative phasing. Coordination mode is indicated by the relative phasing of the ipsilateral HN(4) and HN(7) interneurons. Across the switch the HE(8) motor neuron does not shift phase with respect to the ipsilateral HN(4) phase reference.

Bilateral phase diagrams of motor neuron firing with respect to the HN(4) interneurons were used to illustrate phase relations between heart interneurons and heart motor neurons. A vertical line that bisects each phase box near its midpoint indicates the mean phase for each heart interneuron. The beginning and end of each box indicate the average time of the first and last spikes, respectively, in a series of bursts relative to the middle spike time of the absolute phase reference cell. Error bars indicate the SD around the mean first, middle, and last spike in a burst.

For the heart motor neurons we also calculated intraburst spike frequency. Each interspike interval in a burst was converted to a frequency (reciprocal) and the maximum, minimum, and average of these frequencies were then averaged across bursts and reported as maximum spike frequency (F_{max}), minimum spike frequency (F_{min}), and mean spike frequency (F), respectively.

Means are presented ± SD.

RESULTS

Our present aim was to characterize as quantitatively as possible the firing pattern of segmental heart motor neurons and their phase relations with the premotor heart interneurons and to complement our previous quantitative description of the firing pattern and phase relations of premotor heart interneurons (Norris et al. 2006). Specifically, we determined directly the bilateral (absolute) phase relations of the HE(3)–HE(18)

motor neurons with the HN(4) heart interneurons and were thereby able to anchor the previously described fictive motor pattern (Wenning et al. 2004b) to the previously described activity pattern of the premotor interneuron in the heartbeat CPG (Norris et al. 2006). We thus assessed how the synaptic output of the heartbeat CPG is transformed into the heartbeat fictive motor pattern.

Relative phasing of premotor heart interneurons and heart motor neurons

Here we establish the relative phasing of the premotor interneurons of the heartbeat CPG with the motor neurons permitting a more precise description of how input (interneuron pattern) is transformed to output (motor neuron pattern). Our method was simple; the HN(4) heart interneuron acts as a phase reference for the heart interneuron pattern and the ipsilateral HN(7) interneuron as an indicator of the ipsilateral coordination mode of the heartbeat CPG. In 61 different preparations, we recorded these two neurons extracellularly and, in addition, recorded extracellularly a series of segmental heart motor neurons one or two at a time; motor neuron phase was measured with respect to the HN(4) interneuron phase reference (0.0 phase peristaltic and 0.511 synchronous) in both coordination modes.

Figure 2 illustrates the method of recording relative phasing of interneurons and motor neurons and typical recordings. In the top panels (Fig. 2*A*), peristaltic coordination in the interneurons (CPG) is mirrored by peristaltic coordination of the motor neurons, and synchronous coordination of the CPG is mirrored by synchronous coordination in the motor neurons. Note that the HE(4) motor neuron is nearly in antiphase with the HN(4) interneuron in synchronous coordination and is nearly in phase with the HN(4) interneuron in peristaltic coordination. The HE(7) motor neuron barely shifts its phase

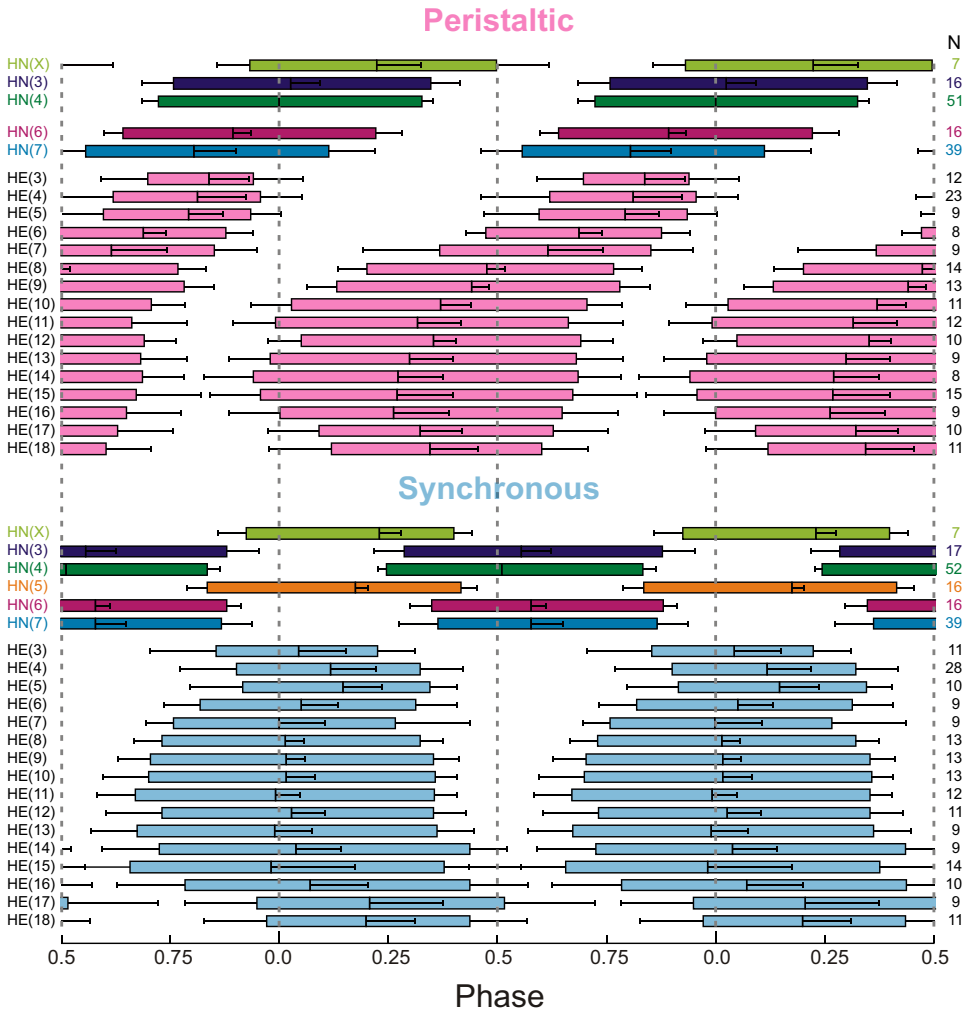

FIG. 5. Summary bilateral phase diagram of the premotor (standard color code) and switch interneurons (orange) of the heartbeat central pattern generator with the entire segmental ensemble of heart motor neurons. Previously (Norris et al. 2006), an ipsilateral phase diagram of the interneurons was constructed from measurements of activity phase relative to the ipsilateral HN(4) interneuron's middle spike for both synchronous and peristaltic coordination modes. To align the ipsilateral phase diagrams into a bilateral diagram the synchronous HN(4) interneuron was assigned a phase of 0.511, as measured with respect to the peristaltic HN(4) interneuron in bilateral recordings. All other synchronous interneurons were then offset by the same amount as the phase of the synchronous HN(4) interneuron. As described in METHODS, extracellular records of the HE motor neurons in each segment were made with respect to the ipsilateral HN(4) phase reference interneuron in both peristaltic and synchronous coordination mode and the middle spike of their bursts assigned a phase with respect to this phase reference. For both motor neurons and interneurons, the average duty cycle is indicated by the length of the bar: the left edge of each bar indicates the average phase of the first spike of the burst and the right edge indicates the average phase of the last spike of the burst. Average phase is indicated by a vertical line within the bar. Error bars indicate SDs. The switch interneuron [HN(5)] is silent in the peristaltic coordination mode.

across the two coordination modes. The bottom panels (Fig. 2*B*), which illustrates the activity of a rear motor neuron, show that the HE(13) motor neuron, like the HE(4) motor neuron, shows a clear shift in phasing with respect to the ipsilateral HN(4) interneuron across the two coordination modes. Figure 3 shows this shift in the HE(4) motor neuron's phase with respect to the ipsilateral HN(4) interneuron across a switch in coordination mode. The HE(3) motor neuron likewise shows a clear shift in phase but less so than the HE(4) motor neuron. Recordings like those in Figs. 2 and 3 led to the prediction that phase shifts increase frontward from the HE(8) motor neuron, reaching a maximum at the HE(4) motor neuron and then falling back somewhat at the HE(3) motor neuron and rearward of the HE(8) motor neuron, the HE(8) motor neuron being a fixed point. This fixed point prediction is consistent with the observations that the HE(8) motor neurons are antiphasic and do not shift relative to one another across a switch in coordination mode (Wenning et al. 2004b). This prediction is realized in the recordings of Fig. 4.

Figure 5 is a summary diagram of phase and duty cycle that combines the activity phase/duty cycle diagram of the premotor and switch interneurons and the motor neuron activity phase/duty cycle. The motor neuron pattern illustrated here derives from the current experiments, whereas the interneuron pattern is that of Norris et al. (2006); the interneuron recordings here were used exclusively as phase references [HN(4) interneurons] for the motor neurons and indicators of coordination mode [HN(7) interneurons]. Although the motor neuron activity pattern was derived independently, it recapitulates the motor neuron activity pattern of Wenning et al. (2004b) derived from extracellular recordings of the heart motor neuron axons in peripheral nerve branches. Table 1 presents the motor neuron data of Fig. 5 in tabular form and also includes measurements of intraburst spike frequency for each motor neuron in both peristaltic and synchronous coordination modes.

Animal-to-animal variability in the phase relations of heart motor neurons and heart interneurons

By presenting average data in Fig. 5, we portray a stereotypical fictive motor program and its coordination with its premotor inhibitory inputs. How well do the average data convey the actual stereotypy, i.e., what is the range of phase variation in the fictive motor program? How does this variability in fictive motor program compare with the phase variability in the CPG output? To approach these questions we plotted the unpacked (in the sense that we retrieved the individual data

TABLE 1. *Intraburst spike frequency [mean (F), maximum (F_{max}) minimum (F_{min})], phase (middle, first, last spikes), and duty cycle (D) for all heart motor neurons [HE(3)–HE(18)] in both coordination modes, peristaltic (PERI) and synchronous (SYNC)*

		Spike Frequency						Spike Phase							
HE	*n*	Mean	SD	Maximum	SD	Minimum	SD	Middle	SD	First	SD	Last	SD	Duty Cycle	*n*
PERI															
HE(3)	12	9.6	4.2	17.6	9.0	3.9	1.5	0.84	0.09	0.70	0.11	0.94	0.11	0.24	12
HE(4)	23	7.5	3.4	12.6	7.7	3.2	0.7	0.81	0.11	0.62	0.16	0.96	0.10	0.34	23
HE(5)	9	7.8	2.7	13.1	5.6	2.9	0.6	0.79	0.08	0.60	0.13	0.94	0.07	0.34	9
HE(6)	8	8.1	2.0	13.1	3.8	3.5	0.7	0.69	0.05	0.47	0.04	0.88	0.06	0.40	8
HE(7)	9	7.8	2.0	13.8	4.9	2.7	0.6	0.62	0.13	0.37	0.18	0.85	0.10	0.48	9
HE(8)	14	9.1	2.0	17.2	5.3	3.1	0.4	0.47	0.04	0.20	0.07	0.77	0.07	0.57	14
HE(9)	13	8.3	2.0	15.9	4.7	2.8	0.4	0.44	0.04	0.13	0.07	0.78	0.07	0.65	13
HE(10)	11	9.1	1.7	17.4	3.8	3.3	0.3	0.37	0.07	0.03	0.09	0.71	0.08	0.68	11
HE(11)	12	8.2	0.3	15.6	1.1	3.2	0.3	0.32	0.10	0.99	0.10	0.66	0.13	0.67	12
HE(12)	10	7.3	1.9	13.0	3.9	3.4	0.6	0.35	0.05	0.05	0.08	0.69	0.07	0.64	10
HE(13)	10	7.3	1.9	13.3	4.0	3.4	0.8	0.30	0.10	0.98	0.10	0.68	0.11	0.70	9
HE(14)	8	7.5	1.2	16.0	3.2	3.2	0.4	0.27	0.10	0.94	0.11	0.69	0.10	0.74	8
HE(15)	15	8.1	2.2	15.7	4.5	3.6	1.3	0.27	0.13	0.96	0.12	0.67	0.15	0.72	15
HE(16)	9	8.7	2.6	17.3	4.8	3.6	0.6	0.26	0.13	0.00	0.12	0.65	0.13	0.65	9
HE(17)	10	7.3	0.4	14.6	1.5	3.0	0.2	0.32	0.10	0.09	0.12	0.63	0.13	0.54	10
HE(18)	11	8.1	1.6	16.1	4.4	3.2	0.4	0.34	0.11	0.12	0.14	0.60	0.10	0.48	11
SYNC															
HE(3)	11	11.8	4.9	23.7	10.5	4.1	1.5	0.04	0.11	−0.15	0.15	0.23	0.08	0.37	11
HE(4)	28	6.5	2.7	11.0	5.6	2.7	0.6	0.12	0.10	−0.10	0.13	0.32	0.10	0.42	28
HE(5)	10	6.1	2.2	10.7	5.1	2.4	0.7	0.15	0.09	−0.08	0.12	0.35	0.06	0.43	10
HE(6)	9	7.6	2.2	13.6	4.0	2.9	0.9	0.05	0.08	−0.18	0.08	0.31	0.09	0.49	9
HE(7)	9	7.3	1.6	11.8	2.7	3.1	0.8	0.00	0.11	−0.24	0.06	0.27	0.17	0.51	9
HE(8)	13	9.6	1.9	18.1	4.8	3.2	0.4	0.01	0.04	0.73	0.06	0.32	0.05	0.59	13
HE(9)	13	8.8	2.1	16.3	4.8	3.1	0.4	0.02	0.04	0.70	0.08	0.35	0.06	0.65	13
HE(10)	13	8.4	2.3	15.4	5.1	3.3	0.5	0.02	0.07	0.70	0.10	0.36	0.05	0.66	13
HE(11)	12	8.2	1.5	16.1	4.0	3.3	0.6	0.99	0.06	0.67	0.09	0.36	0.05	0.69	12
HE(12)	11	7.1	1.8	12.4	4.2	3.2	0.5	0.03	0.08	0.73	0.13	0.35	0.07	0.62	11
HE(13)	10	7.2	1.7	13.1	3.6	3.4	0.9	0.99	0.08	0.67	0.10	0.36	0.08	0.69	9
HE(14)	9	7.7	1.0	15.3	2.9	3.3	0.4	0.04	0.10	0.73	0.13	0.44	0.09	0.71	9
HE(15)	14	8.3	1.8	16.1	4.6	3.8	1.3	0.98	0.19	0.66	0.22	0.38	0.18	0.72	14
HE(16)	10	8.7	2.3	18.1	5.9	3.6	0.6	0.07	0.13	0.78	0.16	0.44	0.13	0.65	10
HE(17)	9	8.5	1.6	16.9	4.1	3.3	0.5	0.21	0.17	0.95	0.17	0.52	0.21	0.57	9
HE(18)	11	8.9	1.4	17.2	3.6	3.8	0.8	0.20	0.11	0.97	0.14	0.44	0.13	0.46	11

Values are means ± SD, except duty cycle. See METHODS.

points that had been used to calculate means) archival (i.e., previously published) data of Fig. 5 on CPG interneuron phase (middle spike) and the unpacked data of Fig. 5 on motor neuron phase (Fig. 6). The phase range of the motor neurons is greater than that of the interneuronal inputs: The phase relations of the rearmost motor neurons are particularly variable, especially in the synchronous mode, perhaps reflecting variability in the HN(7) interneurons' activity phases. Least variable are midbody motor neurons with the main peristaltic phase progression from the HE(13) to the HE(5) motor neuron being most stereotypical among preparations. Thus any model of motor neuron coordination in this system should capture this phase progression well. The frontmost HE(3) and HE(4) motor neurons are highly variable in both modes, which fits well with variability of the HN(X) interneuron's phasing in the peristaltic mode but not with its relative constancy in the synchronous mode, but then the HN(3) interneurons are remarkably variable in their activity phases.

Bilateral coordination of the heart motor neurons

The summary diagram of Fig. 5, derived from unilateral recordings, indicates that the bilateral HE(4) motor neurons should show a short duty cycle, with one following the other closely in phase and the HE(4) motor neuron on the peristaltic side leading slightly. Moreover, the diagram shows that the bilateral HE(7) motor neurons should show a long duty cycle and be active nearly in antiphase to each other. The bilateral motor neuron recordings of Fig. 7 support these indications.

DISCUSSION

Here we systematically measured the phase relations (relative coordination) between the activity pattern of premotor heart interneurons and the activity pattern of the heart motor neurons, thus unifying the fictive motor pattern with fictive CPG activity. To extract insights from this analysis we address three questions.

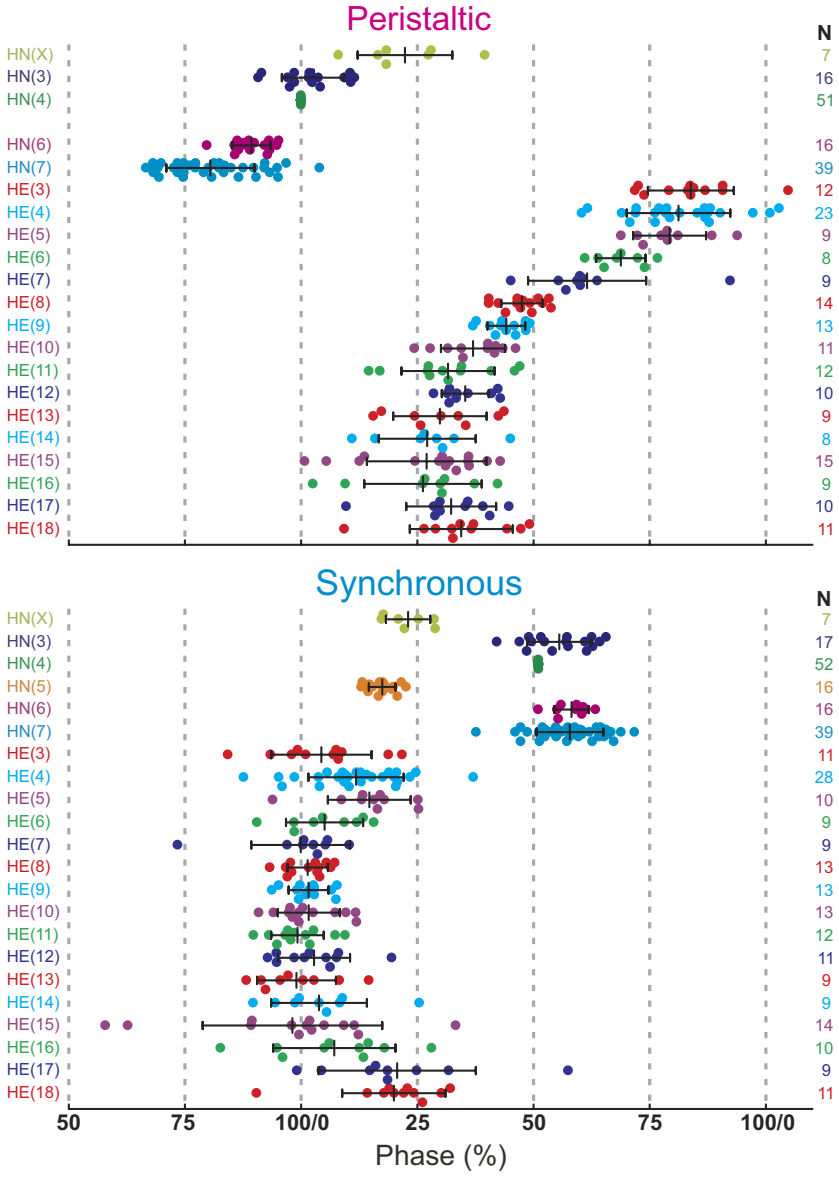

FIG. 6. Variability in heart interneuron and heart motor neuron coordination. Bilateral summary diagram showing average phase (middle spike) ± SD (black bars) from Fig. 5 and individual values (colored dots) and number of values (*n*), each corresponding to a different animal, used to compute these averages. Motor neuron data are from the current experiments and the interneuron data are archival from Norris et al. (2006). Colors for the interneurons corresponds to code of Fig. 1, but colors for the motor neurons are arbitrary.

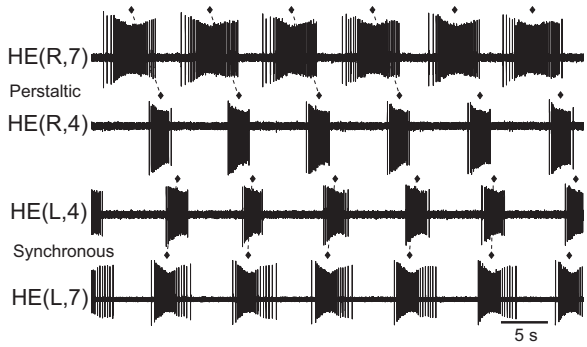

FIG. 7. Bilateral coordination of HE(4) and HE(7) heart motor neurons. Shown are bilateral extracellular recordings from HE(4) and HE(7) heart motor neurons with the right side in the peristaltic and the left side in the synchronous coordination mode. Black diamonds indicate the middle spike of each burst and dashed lines are provided to facilitate observation of relative phasing. Coordination mode is indicated by the relative phasing of the ipsilateral HE(4) and HE(7) motor neurons.

Is the coordination of the fictive pattern of heart motor neuron activity stereotypical?

The summary phase diagram of Fig. 5 and the numerical average data in Table 1 suggest an affirmative answer, especially considering the moderate SDs found in the data set. It is perhaps more revealing to see how individual preparations fall in the bands defined by the SDs. This view suggests that the SD values are good indicators of variability and that the midbody motor neurons are most tightly coordinated to CPG output and thus show the most consistent intersegmental coordination—especially the phase progression of the HE(13)–HE(5) motor neurons in peristaltic coordination mode appear tightly regulated. Thus any model of motor neuron coordination in this system should focus on this feature as a criterion for matching the living system. Corresponding motor neurons in synchronous coordination mode appear less closely coordinated to the CPG but only slightly so. Frontmost and rearmost motor neurons are quite flexible in the phasing with respect to their premotor inputs (Fig. 6).

In a similar study of variability in a CPG and associated motor neurons, Bucher et al. (2005) concluded that in the pyloric CPG of the lobster (*Homarus americanus*) mean phase relations were relatively tightly maintained across preparations and might represent the set point of homeostatic regulation. The phase variability we observed here is comparable. This phase tolerance observed in two different CPGs, if it indeed results from homeostatic regulation, would suggest that the set points of such regulation, at least at the network level, are broad.

How does the variability in the fictive motor program compare with the constriction pattern of the hearts?

Figure 8 presents unpacked archival data from Wenning et al. (2004a) on the phasing of systole in intact leeches using systole in the peristaltic heart in segment 10 as a phase reference. In general, variability is greater in the constriction pattern than in the fictive motor pattern: as in the fictive motor program the coordination of the rearmost heart segmental sections is highly variable, especially in segmental sections 14–16 in the synchronous heart. Segmental sections 3 and 4 are highly variable in both the peristaltic and the synchronous heart, as in the fictive motor program. The phase progression for the midbody segmental sections in the peristaltic heart is highly stereotyped as in the fictive motor program, but in the synchronous heart, it is more variable and less synchronous in appearance than the fictive motor program. The synchronous heart does convey a front-to-rear progression not observed in the fictive motor program where there is near synchrony. The synchronous heart does support rearward blood flow along its length (Wenning and Meyer 2007), a fact not apparent from the fictive motor pattern.

Is the middle spike of a burst a useful maker for activity phase in a fictive motor pattern?

The data of Table 1 show that across different animals middle spike phase consistently has a lower SD than that of either first spike phase or last spike phase. Similarly as with heart interneurons (Hill et al. 2001; Masino and Calabrese 2002c; Norris et al. 2006), the middle spike phase has a lower SD within a preparation (data not shown). These observations thus indicate that the middle spike phase is not only ideal for characterizing the motor pattern quantitatively and constraining any potential model of heart motor neuron coordination, but also might be more closely regulated by the nervous system.

Can the output of the central pattern generator be translated into the fictive motor pattern?

Our ultimate goal is to construct a model that will translate the fictive output of the heartbeat central pattern generator into the fictive heartbeat motor pattern. This goal drove us to define as accurately as possible the phase relations between the CPG firing pattern and the motor neuron firing pattern presented here. Although there is considerable variability in both the

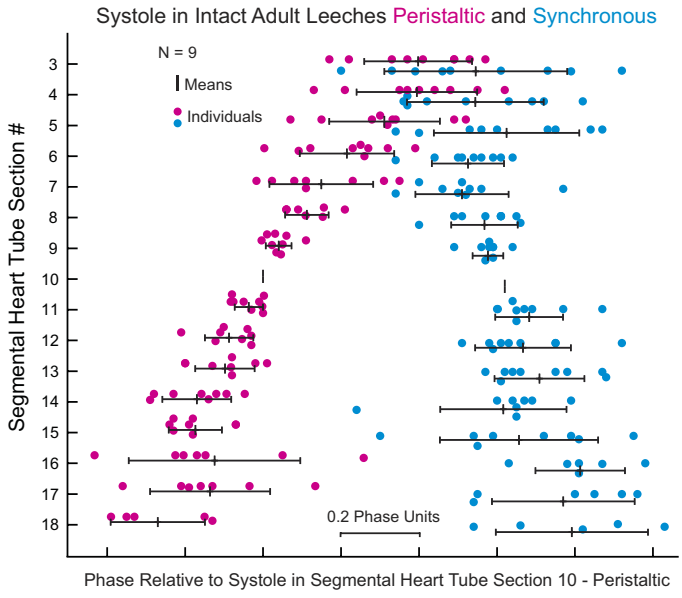

FIG. 8. Variability in heart constriction pattern: intersegmental coordination of systole. Bilateral summary diagram showing average phase (middle spike) ± SD (black bars) archival data from Wenning et al. (2004a), Fig. 5, and individual values (pink dots peristaltic, light blue dots synchronous)—8 values (*n*), each corresponding to a different animal—used to compute these averages.

phase relations of the fictive motor program and of the CPG (premotor) activity pattern, we have been able to identify stereotypical features, e.g., the rear-to-front phase progression of midbody motor neurons in the peristaltic coordination mode that any model must capture, if it is to illuminate underlying mechanisms. In a subsequent paper we explore the synaptic weights, synaptic plasticity, and conduction delays that characterize the linkage between the interneurons and motor neurons in the leech heartbeat system.

ACKNOWLEDGMENTS

Present address of A. L. Weaver: Department of Biology, Xavier University of Louisiana, New Orleans, LA 70125.

GRANTS

This work was supported by National Institute of General Medical Sciences National Research Service Award Institutional Research and Academic Career Development postdoctoral fellowship GM-000680 to A. L. Weaver and by National Institute of Neurological Disorders and Stroke Grant NS-24072 to R. L. Calabrese.

REFERENCES

Bucher D, Prinz AA, Marder E. Animal-to-animal variability in motor pattern production in adults and during growth. *J Neurosci* 25: 1611–1619, 2005.

Bucher D, Taylor AL, Marder E. Central pattern generating neurons simultaneously express fast and slow rhythmic activities in the stomatogastric ganglion. *J Neurophysiol* 95: 3617–3632, 2006.

Calabrese RL. The neural control of alternate heartbeat coordination states in the leech, *Hirudo medicinalis. J Comp Physiol* 122: 111–143, 1977.

Calabrese RL. The roles of endogenous membrane properties and synaptic interaction in generating the heartbeat rhythm of the leech, *Hirudo medicinalis*. *J Exp Biol* 82: 163–176, 1979.

Calabrese RL, Peterson E. Neural control of heartbeat in the leech, *Hirudo medicinalis*. *Symp Soc Exp Biol* 37: 195–221, 1983.

Cang J, Friesen WO. Model for intersegmental coordination of leech swimming: central and sensory mechanisms. *J Neurophysiol* 87: 2760–2769, 2002.

De Schutter E, Ekeberg O, Kotaleski JH, Achard P, Lansner A. Biophysically detailed modelling of microcircuits and beyond. *Trends Neurosci* 28: 562–569, 2005.

Gramoll S, Schmidt J, Calabrese RL. Switching in the activity state of an interneuron that controls coordination of the hearts in the medicinal leech (*Hirudo medicinalis*). *J Exp Biol* 186: 157–171, 1994.

Grillner S, Markram H, De Schutter E, Silberberg G, LeBeau FE. Microcircuits in action—from CPGs to neocortex. *Trends Neurosci* 28: 525–533, 2005.

Hildebrandt J-P. Circulation in the leech, *Hirudo medicinalis. J Exp Biol* 134: 235–246, 1988.

Hill AA, Lu J, Masino MA, Olsen OH, Calabrese RL. A model of a segmental oscillator in the leech heartbeat neuronal network. *J Comput Neurosci* 10: 281–302, 2001.

Hill AA, Masino MA, Calabrese RL. Model of intersegmental coordination in the leech heartbeat neuronal network. *J Neurophysiol* 87: 1586–1602, 2002.

Jezzini SH, Hill AA, Kuzyk P, Calabrese RL. Detailed model of intersegmental coordination in the timing network of the leech heartbeat central pattern generator. *J Neurophysiol* 91: 958–977, 2004.

Kiehn O. Locomotor circuits in the mammalian spinal cord. *Annu Rev Neurosci* 29: 279–306, 2006.

Krahl B, Zerbst-Boroffka I. Blood-pressure in the leech *Hirudo medicinalis*. *J Exp Biol* 107: 163–168, 1983.

Kristan WB Jr, Calabrese RL, Friesen WO. Neuronal control of leech behavior. *Prog Neurobiol* 76: 279–327, 2005.

Lu J, Gramoll S, Schmidt J, Calabrese RL. Motor pattern switching in the heartbeat pattern generator of the medicinal leech: membrane properties and lack of synaptic interaction in switch interneurons. *J Comp Physiol A Sens Neural Behav Physiol* 184: 311–324, 1999.

Maranto AR, Calabrese RL. Neural control of the hearts in the leech, *Hirudo medicinalis.* I. Anatomy, electrical coupling, and innervation of the hearts. *J Comp Physiol A Sens Neural Behav Physiol* 154: 367–380, 1984a.

Maranto AR, Calabrese RL. Neural control of the hearts in the leech, *Hirudo medicinalis*. II. Myogenic activity and its control by heart motor neurons. *J Comp Physiol A Sens Neural Behav Physiol* 154: 381–391, 1984b.

Marder E, Bucher D. Understanding circuit dynamics using the stomatogastric nervous system of lobsters and crabs. *Annu Rev Physiol* 69: 291–316, 2007.

Marder E, Bucher D, Schulz DJ, Taylor AL. Invertebrate central pattern generation moves along. *Curr Biol* 15: R685–R699, 2005.

Marder E, Calabrese RL. Principles of rhythmic motor pattern generation. *Physiol Rev* 76: 687–717, 1996.

Marder E, Goaillard JM. Variability, compensation and homeostasis in neuron and network function. *Nat Rev Neurosci* 7: 563–574, 2006.

Masino MA, Calabrese RL. A functional asymmetry in the leech heartbeat timing network is revealed by driving the network across various cycle periods. *J Neurosci* 22: 4418–4427, 2002a.

Masino MA, Calabrese RL. Period differences between segmental oscillators produce intersegmental phase differences in the leech heartbeat timing network. *J Neurophysiol* 87: 1603–1615, 2002b.

Masino MA, Calabrese RL. Phase relationships between segmentally organized oscillators in the leech heartbeat pattern generating network. *J Neurophysiol* 87: 1572–1585, 2002c.

Mulloney B, Hall WM. Local and intersegmental interactions of coordinating neurons and local circuits in the swimmeret system. *J Neurophysiol* 98: 405–413, 2007.

Mulloney B, Harness PI, Hall WM. Bursts of information: coordinating interneurons encode multiple parameters of a periodic motor pattern. *J Neurophysiol* 95: 850–861, 2006.

Norris BJ, Weaver AL, Morris LG, Wenning A, Garcia PA, Calabrese RL. A central pattern generator producing alternative outputs: temporal pattern of premotor activity. *J Neurophysiol* 96: 309–326, 2006.

Siddall ME, Trontelj P, Utevsky SY, Nkamany M, Macdonald KS. Diverse molecular data demonstrate that commercially available medicinal leeches are not Hirudo medicinalis. *Proc Biol Sci* 274: 1481–1487, 2007.

Thompson WJ, Stent GS. Neuronal control of heartbeat in the medicinal leech. I. Generation of the vascular constriction rhythm by heart motor neurons. *J Comp Physiol* 111: 261–279, 1976a.

Thompson WJ, Stent GS. Neuronal control of heartbeat in the medicinal leech. II. Intersegmental coordination of heart motor neuron activity by heart interneurons. *J Comp Physiol* 111: 281–307, 1976b.

Thompson WJ, Stent GS. Neuronal control of heartbeat in the medicinal leech. III. Synaptic relations of the heart interneurons. *J Comp Physiol* 111: 309–333, 1976c.

Wenning A, Cymbalyuk GS, Calabrese RL. Heartbeat control in leeches. I. Constriction pattern and neural modulation of blood pressure in intact animals. *J Neurophysiol* 91: 382–396, 2004a.

Wenning A, Hill AA, Calabrese RL. Heartbeat control in leeches. II. Fictive motor pattern. *J Neurophysiol* 91: 397–409, 2004b.

Wenning A, Meyer EP. Hemodynamics in the leech: blood flow in two hearts switching between two constriction patterns. *J Exp Biol* 210: 2627–2636, 2007.